

# Design and Applicability of Multi-Core Fibers With Standard Cladding Diameter

Takashi Matsui , Yuto Sagae , Taiji Sakamoto , and Kazuhide Nakajima , *Member, IEEE*

**Abstract**—We show the design and applicability of multi-core fiber (MCF) with the standard 125  $\mu\text{m}$  cladding diameter to the telecommunication systems. It offers easier and practical use of the space-division multiplexing (SDM) technology given its excellent fiber productivity and utilization of existing standard technologies. We numerically and experimentally reveal that the simple step-index (SI) profile enables us to allocate four cores in the standard 125  $\mu\text{m}$  cladding and to realize full compliance with G.657.A1 fiber. We then expand the design and concept of the standard cladding MCF and show the index profile and single-mode bandwidth offer control of XT characteristics. We elucidate the application scope of the standard cladding MCF for not only the full-band (O-L band) application to short-reach and terrestrial transmission consistent with ITU-T Recommendations G.652 and G.657, but also ultra-long haul transmission, such as submarine systems compliant with ITU-T Recommendation G.654.

**Index Terms**—Micro-bending, multi-core fiber, space division multiplexing.

## I. INTRODUCTION

SPACE division multiplexing (SDM) technology is a promising approach to overcoming the 100 Tbit/s capacity limitation of conventional single-mode fiber (SMF). SDM can be classified into core division multiplexing on a multi-core fiber (MCF) and mode division multiplexing (MDM) on a multi-mode fiber (MMF). SDM transmission at above 100 Tbit/s was reported in 2011 for the first time by using 7-core fiber with cladding diameter of 150  $\mu\text{m}$  [1], and much higher capacity transmission experiments such as beyond 1 Pbit/s and 1 Ebit/s-km transmission were achieved by utilizing single-mode MCFs (SM-MCFs) [2]–[5]. Combining MCF with MMF, namely the multi-mode MCF (MM-MCF), enables us to greatly increase the number of spatial channels to 100 or more [6]–[9] and 10 Pbit/s transmission was demonstrated by using MM-MCF that supported 114 spatial channels [10]. However, MDM transmission requires much complex digital signal processing of the multi-input multi-output, and ASIC implementation is deemed to be infeasible given current semiconductor technology.

Manuscript received March 11, 2020; revised May 29, 2020; accepted June 22, 2020. Date of publication June 25, 2020; date of current version November 1, 2020. A part of this work was supported by the National Institute of Information Communication Technology (NICT) Japan. (*Corresponding author: Takashi Matsui.*)

The authors are with the NTT Access Network Service Systems Laboratories, Nippon Telegraph and Telephone Corporation, Ibaraki 305-0805, Japan (e-mail: takashi.matsui.uh@hco.ntt.co.jp; yuuto.sagae.nm@hco.ntt.co.jp; taiji.sakamoto.un@hco.ntt.co.jp; kazuhide.nakajima.gr@hco.ntt.co.jp).

Color versions of one or more of the figures in this article are available online at <https://ieeexplore.ieee.org>.

Digital Object Identifier 10.1109/JLT.2020.3004824

Although many SM-MCF structures have been proposed that set more than 10 cores in one fiber, their cladding is thicker than the standard 125  $\mu\text{m}$  cladding diameter. The thicker cladding directly degrades fiber productivity. The required preform size is proportional to the square of the cladding diameter. For example, to fabricate a 1000 km-long MCF with 250  $\mu\text{m}$  cladding diameter, a preform length of 4 m and diameter of 120 mm is needed. Obviously it is impractical to fabricate such large fiber preforms with current fiber fabrication processes and the highly uniform placement of core rods needs an innovative fiber fabrication process. Recently, MCFs with standard cladding have been proposed to not only improve the fiber productivity but also utilize the existing optical cables and connector interfaces. Moreover, optical compatibility with the current SMF standards would enable us to utilize conventional optical components. It has been reported that the standard cladding diameter of 125  $\mu\text{m}$  supports four homogeneous cores [11] and five heterogeneous cores [12] and sufficiently low inter-core crosstalk (XT) is possible with the trench-assisted index profile.

Interconnectivity among standard cladding MCFs fabricated from several manufacturers was demonstrated for the first time in 2017 and transmission in excess of 100 Tbit/s was successfully achieved over a 316 km full SDM link composed of standard cladding MCFs [13], highly efficient MC-EDFAs [14]–[16] and MCF connectors [17], [18]. The experiments also indicated that a four-core fiber with trench-assisted profile fully compatible with SMF could achieve 100 Pbit/s-km transmission [19]. Moreover, to extend the transmission distance to several thousands of km, the standard cladding MCF with limited single-mode bandwidth in the low-loss C+L band was proposed and demonstrated [20]–[22]. We have recently investigated the applicability of the step-index (SI) profile to the standard cladding MCF (SI-MCF) since this profile is widely used for conventional G.652.D fiber and has the great advantage of supporting mass production by the VAD method; the full-band applicability of SI-MCF to terabit/s class transmission over distances of several tens of km has been shown [23], [24].

This paper elucidates the design and potential of the standard cladding MCF by considering its optical compatibility with conventional fiber standards. First, we numerically and experimentally investigate the design and characteristics of SI-MCF with standard cladding diameter that offers optical compatibility with conventional G.657.A1 fibers. The applicability of SI-MCF to conventional optical fiber cables is also shown in terms of the micro-bending sensitivity of its loss increase and XT variation. We then investigate the upgradability of the standard cladding

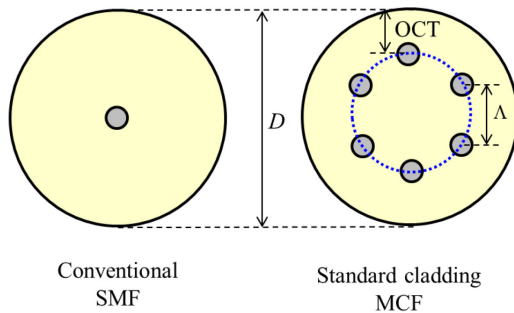


Fig. 1. Concept of standard cladding MCF.

MCF by considering its transmission distance and single-mode bandwidth as well as the optical compatibility with several existing standards. We consider the refractive index profile of the SI, trench-assisted and depressed cladding profiles, and the two types of single-mode bandwidth that is O-L band and C+L band, and we show that standard cladding MCFs can be designed and optimized while satisfying the XT requirements in various application areas and compliance with ITU-T Recommendations G.652, 654 and 657 simultaneously.

## II. STANDARD CLADDING MCF WITH SI PROFILE FOR FULL-BAND APPLICATION

Fig. 1 shows the concept of our proposed standard cladding MCF [11]. As it adopts the standard cladding diameter,  $D$ , of  $125 \pm 0.7 \mu\text{m}$ , we can expect both improved fiber productivity and the continued use of standard technologies such as the conventional cable structure and optical connector interfaces. Moreover, its optical compatibility with conventional SMF enable MCF links to coexist with traditional SMF links.

At first, we consider the SI profile for the core since this profile is widely used for conventional G.652.D fiber. We consider the optical compatibility of each core with G.652.D and G.657.A1 fibers, which have mode field diameter (MFD) of  $8.6\text{--}9.2 \mu\text{m}$  at a wavelength  $\lambda$  of  $1310 \text{ nm}$ , bending loss  $\alpha_b$  of less than  $0.1 \text{ dB/turn}$  at  $\lambda = 1625 \text{ nm}$  and bending radius  $R$  of  $15 \text{ mm}$ , and a cut-off wavelength  $\lambda_c$  of less than  $1260 \text{ nm}$ . Here, we assume that the SI-MCF has a homogeneous core structure and the cores have a circular arrangement as shown in Fig. 1.

Fig. 2 shows the calculated excess loss and XT of the standard cladding MCF with SI profile (SI-MCF). We set the core diameter,  $2a$ , and relative index difference,  $\Delta$ , to  $8.2 \mu\text{m}$  and  $0.39\%$ , respectively, to maximize the optical confinement; this yielded the MFD of  $8.6 \mu\text{m}$  at  $\lambda = 1310 \text{ nm}$  and the cut-off wavelength  $\lambda_c$  of  $1260 \text{ nm}$ . Fig. 2(a) plots the excess loss,  $\alpha_{ex}$ , as a function of core pitch for different number of cores  $N$ ; loss was calculated as the confinement loss at  $\lambda = 1625 \text{ nm}$ . The black, red, blue and green represent  $N = 3, 4, 5$  and  $6$  respectively. Because of the fixed cladding diameter  $D = 125 \mu\text{m}$ , the outer cladding thickness (OCT) reduced as given by  $\text{OCT} = D/2 - \Lambda/(2 \sin(\pi/N))$ , and  $\alpha_{ex}$  increased when core pitch  $\Lambda$  and/or the number of the cores increased. Here, we considered to reduce  $\alpha_{ex}$  to less than  $0.01 \text{ dB/km}$ , which corresponded to the one-order smaller value than the propagation loss of the conventional SMF.  $\Lambda$  had to be smaller than  $47, 38,$

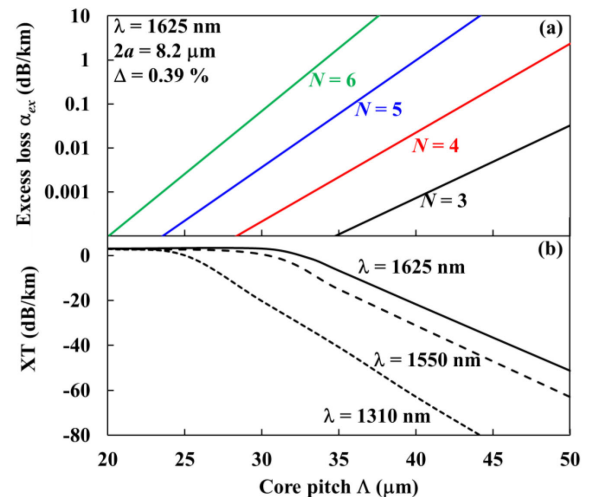


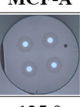
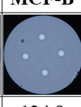
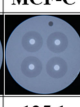
Fig. 2. Design of SI-MCF with standard cladding diameter. (a) is the excess loss as a function of the number of cores, and (b) is the calculated total XT.

$32$  and  $27 \mu\text{m}$  for  $N = 3, 4, 5$  and  $6$ , respectively. Fig. 2(b) plots the XT calculated as the summation of the interference from the neighboring two cores. The XT reached  $0 \text{ dB/km}$  and saturated to  $3 \text{ dB}$  for  $\Lambda \leq 33 \mu\text{m}$  at a wavelength of  $1625 \text{ nm}$ , which resulted in strong coupling among cores and made difficult to transmit signals across each core independently. Up to four SI cores could be allocated in the standard  $125 \mu\text{m}$  cladding diameter while suppressing  $\alpha_{ex}$  sufficiently. For  $N = 4$  with  $\Lambda = 38 \mu\text{m}$ , although the total XT was relatively high at  $-20 \text{ dB/km}$  at  $\lambda = 1625 \text{ nm}$ , the XT was reduced to  $-28 \text{ dB/km}$  and  $-56 \text{ dB/km}$  at  $\lambda = 1550$  and  $1310 \text{ nm}$ , respectively, which enabled us to realize SDM transmission over distances of  $10 \text{ km}$  or longer with the low XT penalty of less than  $1 \text{ dB}$  for QPSK format [25]. This performance numerically revealed that the four homogeneous SI cores could be carried by the standard cladding MCF while maintaining optical compatibility with G.652.D and G.657.A1 fibers.

We then fabricated lengths of SI-MCF and experimentally investigated its optical characteristics. Table I provides cross-sectional photos and measured geometrical and optical properties. Three SI-MCFs were fabricated from three different preforms; each had sufficient volume to create at least  $150 \text{ km}$  fiber. Cladding diameter and core pitch  $\Lambda$  were well controlled to  $125 \mu\text{m}$  and  $40 \mu\text{m}$  (average), respectively. The deviation in  $\Lambda$  was  $0.3 \mu\text{m}$  among the three SI-MCFs, which corresponds to the splice loss of less than  $0.1 \text{ dB}$  at  $\lambda = 1310 \text{ nm}$  given the rotational misalignment of  $0.6$  degrees. The propagation loss was sufficiently low at less than  $0.20 \text{ dB/km}$  at  $\lambda = 1550 \text{ nm}$  for the three SI-MCFs, which is comparable with conventional SMF values. The MFD, cable cut-off wavelength  $\lambda_{cc}$  (at a length of  $22 \text{ m}$ ), bending loss  $\alpha_b$  and zero-dispersion wavelength  $\lambda_0$  were compatible with G.652.D and/or G.657.A1 fiber. We also observed sufficiently low PMD of less than  $0.1 \text{ ps}/\sqrt{\text{km}}$  for all fabricated SI-MCFs.

Fig. 3 plots the measured loss and XT characteristics. Fig. 3(a) shows the loss spectra of the three SI-MCFs. The red, blue and green solid curves represent the average loss among the

TABLE I  
PROPERTIES OF FABRICATED SI-MCFs

| Parameters                                   | $\lambda$ (nm) | Target        | MCF-A   | MCF-B   | MCF-C   |
|--|----------------|---------------|---|---|---|
|  | -              | -             |  |  |  |
| Cladding diameter ( $\mu\text{m}$ )          | -              | $125 \pm 0.7$ | 125.0   | 124.9   | 125.1   |
| Core pitch $\Lambda$ ( $\mu\text{m}$ )       | -              | $40 \pm 1.0$  | 39.7  | 39.9  | 40.0  |
| Loss (dB/km)                                 | 1550           | $< 0.30$      | 0.195   | 0.195   | 0.197   |
| Cable cut-off wavelength $\lambda_{cc}$ (nm) | -              | $< 1260$      | 1242  | 1221  | 1243  |
| MFD ( $\mu\text{m}$ )                        | 1310           | 8.6-9.2       | 8.9   | 8.7   | 9.2   |
| Bending loss $\alpha_b$ (dB/turn)*           | 1625           | $< 0.1$       | $< 0.01$  | $< 0.01$  | $< 0.01$  |
| Zero-dispersion wavelength $\lambda_0$ (nm)  | -              | 1300-1324     | 1310  | 1317  | 1310  |
| PMD (ps/ $\sqrt{\text{km}}$ )                | 1550           | $< 0.2$       | 0.06  | 0.05  | 0.04  |
| Total XT (dB/km)                             | 1625           | -             | -26.7   | -24.6   | -27.4   |
| Fiber length (km)                            | -              | -             | $> 150$ km for each   |   |   |

\*At a bending radius of 15 m.

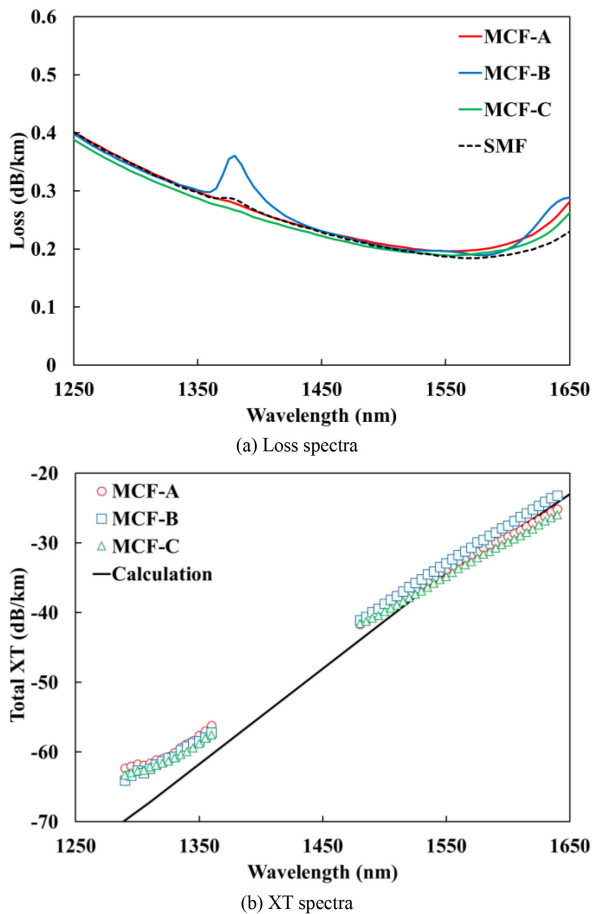


Fig. 3. Measured loss and XT characteristics of three SI-MCFs.

four cores for MCF-A, -B and -C in Table I, respectively. The dashed curve is for a G.657.A1 fiber for comparison. We observed that the SI-MCFs had slightly higher loss than the SMF at  $\lambda > 1600$  nm. It can be considered that the loss difference between the SI-MCFs and the SMF is due to the excess loss since the calculated  $\alpha_{ex}$  was 0.02 dB/km at  $\lambda = 1625$  nm for  $\Lambda = 40$   $\mu\text{m}$  as shown in Fig. 2(a). We also observed the low loss spectra

of less than 0.4 dB/km in full-band for all three SI-MCFs; MCF-B had slightly higher loss at  $\lambda = 1383$  nm due to its OH absorption. Fig. 3(b) plots the total XT characteristics which represents the summation of the interference from the three other cores. The symbols indicate measured values and black line represents the calculated value. The measurement results agreed with the calculated values in the longer wavelength range. The deviation in total XT among the three SI-MCFs was small at less than 2 dB since they had well-controlled  $\Lambda$  and similar optical properties. The XT value was less than  $-33$  dB/km and  $-27$  dB/km at  $\lambda = 1550$  and 1625 nm, respectively, which supports 10~40 km transmission of QPSK format signals with an XT penalty of 1 dB or less over the full-band [25]. We found slightly higher XT than the calculation indicated in the shorter wavelength region; this difference is induced by the XT in the fan-in/fan-out (FIFO) devices. The XT at  $\lambda = 1310$  nm was extremely low at less than  $-62$  dB/km including the FIFO devices, which is expected to have negligible impact on the transmission performance in the O band. In ref. [24], we demonstrated the full-band applicability of SI-MCF to Tera-bit/s class high-speed transmission over the several tens of km; we conducted transmission experiments on both high-speed parallel transmission in the O band and coherent SDM/WDM transmission in the C band.

We then investigated the micro-bending sensitivity of the SI-MCFs to confirm their applicability to conventional optical fiber cables. We prepared 550 m-long test samples of MCF-B and conventional G.652.D and G.657.A1 fibers for comparison. We utilized the wire mesh method to evaluate the micro-bending sensitivity, and controlled the lateral pressure on the fiber by controlling the winding tension applied to the test samples.

Fig. 4 shows the measured micro-bending sensitivity results. Fig. 4(a) shows the loss increase at  $\lambda = 1625$  nm as a function of the applied tension. Solid line corresponds to the average loss increase among the four SI-MCF cores, and the dashed and dotted lines correspond to the G.657.A1 and G.652.D fibers. We found that the SI-MCFs had slightly higher loss increase than the G.657.A1 fiber. It can be considered that the excess loss,  $\alpha_{ex}$ , of the SI-MCF caused the slightly higher micro-bending loss. Compared with the G.652.D fiber, the loss increase was low enough to make SI-MCF suitable for realizing high-density optical fiber cables. Fig. 4(b) shows the change in XT spectrum with lateral pressure. Circles, squares and triangles are for the applied tension values of 0, 1.13 and 1.85 N, respectively, and the solid lines are the linear approximation of the measured results. We observed no significant change in the XT characteristics as the applied tension was increased. Thus, we can expect the lateral pressure induced in the optical fiber cable installation to have negligible impact on the XT characteristics.

These results confirm that our SI-MCF can be used for full-band application while achieving sufficiently low micro-bending sensitivity and full compliance with the G.652.D and G.657.A1 specifications.

### III. UPGRADABILITY OF STANDARD CLADDING MCF

As shown in the previous section, SI-MCF with full-band compatibility with conventional SMF had relatively high XT and thus supported several tens of km transmission. It is known



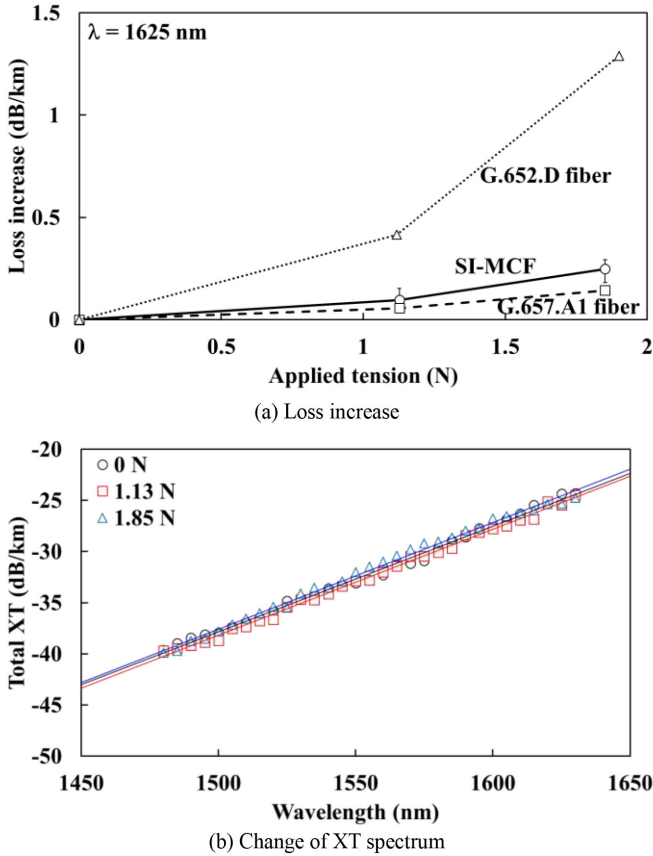


Fig. 4. Micro-bending sensitivity of SI-MCF.

TABLE II  
INDEX PROFILES FOR STANDARD CLADDING MCF

|                           | Full-band  |                              | Cut-off shifted                |
|---------------------------|------------|------------------------------|--------------------------------|
|                           | SI profile | Trench-assisted (TA) profile | Depressed cladding (W) profile |
| Relative index difference |            |                              |                                |

that advanced index profiles such as the trench-assisted (TA) profile can reduce the XT, and the optical properties such as the cut-off wavelength and MFD also affects the XT characteristics. Here, we examined upgrading the standard cladding MCFs to support much longer transmission distances by considering advanced index profiles and the transmission bandwidth. Table II shows the index profiles examined. Here, we considered optical compatibility with the existing fiber standards of G.652, 654.D and 657.A1 fibers. For full-band application, we used the SI and TA profiles. SI profile is widely used for G.652.D fibers because of its mass production capability and uniformity as described above. TA profile is often used for bending-loss insensitive fibers as specified in ITU-T Recommendations G.657 since it has better optical confinement properties. For ultra-long haul transmission

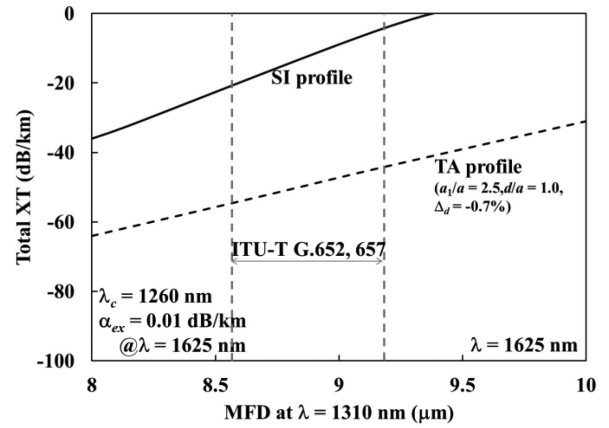


Fig. 5. Relationship between XT and MFD for full-band application.

such as submarine systems, cut-off shifted fiber is used for its low loss and low nonlinear characteristics. The depressed cladding profile, namely W shaped profile, is often used in cut-off shifted fibers as its pure-silica core structure attains large effective areas ( $A_{eff}$ ).

At first, we investigated the XT potential of the standard cladding MCF for full-band application. Fig. 5 shows the relationship between the XT and MFD when considering the optical compatibility with G.652.D and G.657.A1 fibers. The horizontal axis is the MFD at  $\lambda = 1310$  nm, and we set  $\lambda_c = 1260$  nm. Regarding the TA profile, we set the relative position  $a_1/a$  to 2.5, relative width  $d/a$  to 1.0 and depth  $\Delta_d$  to  $-0.7\%$  for the trench structure in order to avoid excessive MFD reduction and to obtain the XT suppression effect [11], [20], [26]. We set the maximum core pitch  $\Lambda$  and minimum OCT to obtain  $\alpha_{ex} = 0.01$  dB/km at  $\lambda = 1625$  nm, which depended on the index profile and optical properties of each core. The large MFD resulted in an increase in XT as expected, and the TA profile improved the XT characteristics by 30 dB or more compared with the SI profile. When we consider the compatible MFD value with G.652 and G.657 fibers, the XT of the SI profile remained  $-20$  dB/km or more and the TA profile offered XT lower than  $-50$  dB/km at  $\lambda = 1625$  nm, which allowed us to realize full-band SDM transmission over distances of hundreds of km.

Here, we can expect to reduce the XT by shifting the cut-off wavelength value to longer wavelengths because of the stronger optical confinement. Fig. 6 shows the XT at  $\lambda = 1625$  nm as a function of the cut-off wavelength. The solid and dashed curves are the SI and TA profiles, respectively; the MFD was  $8.6 \mu\text{m}$  at  $\lambda = 1310$  nm. By lengthening the cut-off wavelength, the XT steadily decreased. For the SI profile, we observed the reduced XT of less than  $-52$  and  $-63$  dB/km by limiting the single-mode bandwidth to the S+C+L and the C+L band, respectively. These values can sufficiently suppress the XT penalty for QPSK format signals in long-distance transmission such as several thousands of km. The TA profile can realize much lower XT,  $-92$  dB/km or less, by shifting the cut-off wavelength to 1460 nm or longer. Therefore, both SI and TA profiles can realize sufficiently low XT for exceeding the 1,000 km-long transmission limits

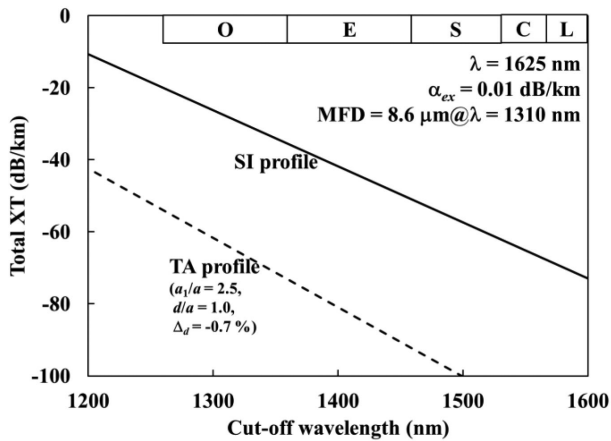


Fig. 6. Relationship between XT and single-mode bandwidth.

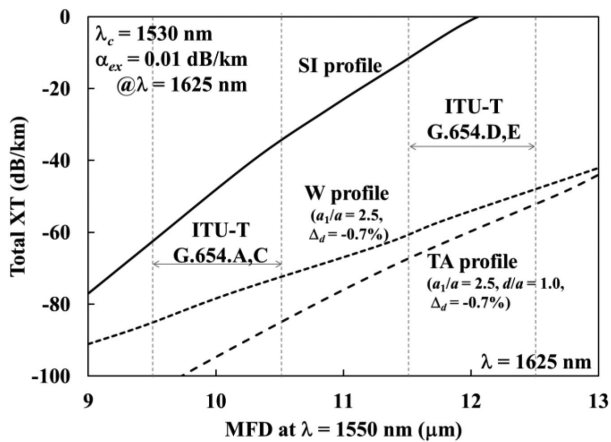


Fig. 7. Relationship between XT and MFD for cut-off shifted type.

of conventional SMF with comparable effective area given its limited single-mode bandwidth.

We then considered expanding the effective area of the standard cladding MCF. Fig. 7 shows the relationship between the XT and the MFD for the cut-off shifted type MCF with  $\lambda_c = 1530$  nm. The horizontal axis is the MFD value at  $\lambda = 1550$  nm. The solid, dashed and dotted curves are the SI, TA and W profiles. We confirmed that the W profile significantly improved the XT characteristics beyond that achieved with the SI profile and TA profile offered larger XT improvement than the W profile. Here, when we consider the XT of less than  $-57$  dB/km, which corresponds to the transmission distance of 10,000 km for the QPSK format, the SI profile realized the MFD of  $9.7 \mu\text{m}$  at  $\lambda = 1550$  nm which is consistent with G.654.A and .C fibers. In contrast, both the W and TA profile realized larger MFD of  $11.7$  and  $12.1 \mu\text{m}$ , respectively, with  $\text{XT} = -57$  dB/km, which are consistent with ITU-T Recommendations G.654.D and .E fibers for a large  $A_{eff}$  cut-off shifted fiber. Therefore, we can expect cut-off shifted type standard cladding MCF will support ultra-long haul transmission and also lower nonlinearity comparable to G.654.E fibers if W or TA profiles are used.

Finally, we summarize the lineup and applicability of standard cladding MCF in Table III. Here, we considered two

TABLE III  
LINEUP AND APPLICABILITY OF STANDARD CLADDING MCF

| Single-mode bandwidth      | Full-band (O-L band)  |             | C+L band             |                       |
|----------------------------|-----------------------|-------------|----------------------|-----------------------|
| Index profile              | SI                    | TA          | SI                   | TA or W               |
| Optically compatible fiber | G.652 and 657 fibers  |             | G.654.A and .C fiber | G.654.D and .E fibers |
| XT potential* (dB/km)      | <-30                  | <-50        | <-60                 |                       |
| Transmission distance (km) | <50                   | 100-1,000   | >1,000               |                       |
| Application area           | Access, metro and DCI | Terrestrial | Submarine            |                       |

\* Achievable XT at  $\lambda = 1550$  nm while suppressing the excess loss and maintaining the optical compatibility with standard fibers.

single-mode bandwidths, full-band (O-L band) and the low-loss C+L band, and optical compatibility with existing fiber standards for telecommunication systems. SI-MCF supports full-band transmission distances of several tens of km while realizing optical compatibility with G.652.D and G.657.A1 fibers. This corresponds to short-reach transmission including access and metro networks and data-center interconnection (DCI). MCF with the TA profile can enhance the transmission distance to several hundreds of km, i.e. high capacity terrestrial networks. By limiting the single-mode bandwidth to the low-loss C+L band, SI-MCF can offer thousands of km transmission and reach to 10,000 km for submarine systems while matching the MFD of conventional SMF (consistent with G.654.A and .C fibers). The TA or W-shaped profile can expand  $A_{eff}$  and improve nonlinearity performance to equal G.654.D and .E fibers while maintaining low enough XT characteristics to suit submarine systems. Therefore, we can expect the standard cladding MCF to be applied to various transmission systems given its excellent performance and optical compatibility with existing fiber standards.

#### IV. CONCLUSION

We showed the concept and application area of standard cladding MCF by considering full optical compliance to existing fiber standards. At first, we revealed that four homogeneous cores with SI profile could be set within the standard cladding diameter; the resulting SI-MCFs were in full compliance with conventional G.657.A1 fiber. Our analysis of the micro-bending sensitivity of the loss and XT confirmed the applicability of SI-MCFs to conventional optical fiber cable structures. We then showed how to upgrade standard cladding MCF performance by using more advanced index profiles such as TA and W profiles and controlling the single-mode transmission bandwidth; the resulting fiber complies with existing standards. For the cut-off shifted type standard cladding MCF (SI profile), the measured XT performance indicated a transmission distance increase to several thousands of km, while use of the TA and W profiles realized both ultra-low XT and large  $A_{eff}$  comparable with G.654.E fiber. We believe that this extensive application range of standard cladding MCFs will greatly encourage the rapid introduction of MCF based SDM transmission systems.

## ACKNOWLEDGMENT

The authors greatly thank Takushi Nagashima, Tetsuya Hayashi, Tetsuya Nakanishi and Tomoki Sano from Sumitomo Electric Industry, Ltd., Katsuhiro Takenaga and Kazuhiko Aikawa from Fujikura, Ltd., Masanori Takahashi, Shinichi Arai, Kazunori Mukasa, Ryuichi Sugizaki and Takeshi Yagi from Furukawa Electric Co., Ltd. and related staffs for their fruitful discussions.

## REFERENCES

- [1] J. Sakaguchi *et al.*, "109-Tb/s ( $7 \times 97 \times 172$ -Gb/s SDM/WDM/PDM) QPSK transmission through 16.8-km homogeneous multi-core fiber," in *Proc. Opt. Fiber Commun. Conf.*, Los Angeles, CA, USA, 2011, Paper PDPB6.
- [2] K. Igarashi *et al.*, "Super-Nyquist-WDM transmission over 7,326-km seven-core fiber with capacity-distance product of 1.03 Exabit/s-km," *Opt. Express*, vol. 22, no. 2, pp. 1220–1228, Jan. 2014.
- [3] H. Takara *et al.*, "1.01-Pb/s (12 SDM/222 WDM/456 Gb/s) Crosstalk-managed transmission with 91.4-b/s/Hz aggregate spectral efficiency," in *Proc. Eur. Conf. Exhib. Opt. Commun.*, Amsterdam, The Netherlands, Sep. 2012, Paper Th3.C.1.
- [4] B. J. Puttnam *et al.*, "2.15 Pb/s transmission using a 22 Core homogeneous single mode multi-core fiber and wideband optical comb," in *Proc. Eur. Conf. Exhib. Opt. Commun.*, Valencia, Spain, Sep. 2015, Paper PDP.3.1.
- [5] T. Kobayashi *et al.*, "1-Pb/s (32 SDM/46 WDM/768 Gb/s) C-band dense SDM transmission over 205.6-km of single-mode heterogeneous multi-core fiber using 96-gbaud PDM-16QAM channels," in *Proc. Opt. Fiber Commun. Conf.*, Anaheim, CA, USA, Mar. 2017, Paper Th5B.1.
- [6] J. Sakaguchi *et al.*, "Realizing a 36-core, 3-mode fiber with 108 spatial channels," in *Proc. Opt. Fiber Commun. Conf.*, Los Angeles, CA, USA, Mar. 2015, Paper Th5C.2.
- [7] K. Igarashi *et al.*, "114 space-division-multiplexed transmission over 9.8-km weakly-coupled-6-mode uncoupled-19-core fibers," in *Proc. Opt. Fiber Commun. Conf.*, Los Angeles, CA, USA, Mar. 2015, Paper Th5C.3.
- [8] T. Sakamoto *et al.*, "Low-loss and low-DMD few-mode multi-core fiber with highest core multiplicity factor," in *Proc. Opt. Fiber Commun. Conf.*, Anaheim, CA, USA, Mar. 2016, Paper Th5A.2.
- [9] T. Sakamoto *et al.*, "120 spatial channel few-mode multi-core fibre with relative core multiplicity factor exceeding 100," in *Proc. Eur. Conf. Exhib. Opt. Commun.*, Roma, Italy, Sep. 2018, Paper We3E.3.
- [10] D. Soma *et al.*, "10.16 Peta-bit/s dense SDM/WDM transmission over Low-DMD 6-Mode 19-Core fibre across C+L Band," in *Proc. Eur. Conf. Exhib. Opt. Commun.*, Gothenburg, Sweden, Sep. 2017, Paper Th.PDPA.1.
- [11] T. Matsui *et al.*, "Design of multi-core fiber in 125  $\mu\text{m}$  cladding diameter with full compliance to conventional SMF," in *Proc. Eur. Conf. Exhib. Opt. Commun.*, Valencia, Spain, Sep. 2015, Paper We.4.3.
- [12] T. Gonda *et al.*, "5-core fiber with heterogeneous design suitable for migration from single-core system to multi-core system," in *Proc. Eur. Conf. Exhib. Opt. Commun.*, Dusseldorf, Germany, Sep. 2016, Paper W.2.B.1.
- [13] T. Matsui *et al.*, "118.5 Tbit/s transmission over 316 km-long multi-core fiber with standard cladding diameter," in *Proc. CLEO-PR/OECC/PGC*, Singapore, Aug. 2017, Paper PDP2.
- [14] H. Ono *et al.*, "12-core double-clad Er/Yb-doped fiber amplifier employing free-space coupling pump/signal combiner module," in *Proc. 39th Eur. Conf. Exhib. Opt. Commun.*, London, U.K., Sep. 2013, Paper We.4.A.4.
- [15] Y. Tsuchida *et al.*, "Cladding pumped seven-core EDFA using an absorption-enhanced erbium doped fibre," in *Proc. 42nd Eur. Conf. Opt. Commun.*, Dusseldorf, Germany, Sep. 2016, Paper M2A.2.
- [16] E. De Gabory *et al.*, "Transmission of 256Gb/s PM-16QAM signal through hybrid cladding and core pumping scheme MC-EDFA controlled for reduced power consumption," in *Proc. Opt. Fiber Commun. Conf. Exhib.*, Mar. 2017, Paper Th1C1.
- [17] K. Sakaime *et al.*, "Mechanical characteristics of MCF connector," in *Proc. IEEE Photon. Soc. SUM*, 2014, pp. 172–173.
- [18] K. Saito *et al.*, "Multi-core fiber connector with precise rotational angle alignment," in *Proc. OECC/ACOFT*, Melbourne, Australia, Jul. 2014, pp. 872–874.
- [19] T. Matsui *et al.*, "Accelerate multi-core fiber application using current standard technology," in *Proc. 23rd Opto-Electron. Commun. Conf.*, Jeju, South Korea, Jul. 2018, Paper 5B2-1.
- [20] Y. Tamura, "Low-loss uncoupled two-core fiber for power efficient practical submarine transmission," in *Proc. Opt. Fiber Commun. Conf. Exhib.*, San Diego, CA, USA, Mar. 2019, Paper M1E.5.
- [21] H. Sakuma *et al.*, "125- $\mu\text{m}$ -cladding low-loss uncoupled four-core fiber," in *Proc. EXAT*, Ise-City, Japan, Mar. 2019, Paper P-13.
- [22] Y. Sagae *et al.*, "Ultra-low-XT multi-core fiber with standard 125- $\mu\text{m}$  cladding for long-haul transmission," in *Proc. 24th OptoElectron. Commun. Conf. Int. Conf. Photon. Switching Comput.*, Fukuoka, Japan, Jul. 2019, Paper TuC3-4.
- [23] T. Matsui and K. Nakajima, "Interconnectivity and high-capacity transmission using multi-core fiber with standard cladding diameter," in *Proc. Opt. Fiber Commun. Conf.*, San Diego, CA, USA, Mar. 2019, Paper Th1I.4.
- [24] T. Matsui *et al.*, "Applicability of step-index type standard cladding multi-core fiber to full-band transmission," in *Proc. Eur. Conf. Exhib. Opt. Commun.*, Dublin, Ireland, Sep. 2019, Paper M.1.D.3.
- [25] P. Winzer *et al.*, "Penalties from in-band crosstalk for advanced optical modulation formats," in *Proc. Eur. Conf. Exhib. Opt. Commun.*, Geneva, Switzerland, Sep. 2011, Paper Tu.5.B.7.
- [26] L.-A. de Montmorillon *et al.*, "All-solid G.652.D fiber with ultra low bend losses down to 5 mm bend radius," in *Proc. Conf. Opt. Fiber Commun./NFOEC*, San Diego, CA, USA, Mar. 2009, Paper OTuI.3.

**Takashi Matsui** received the B.E., M.E., and Ph.D. degrees in electronic engineering from Hokkaido University, Sapporo, Japan, in 2001, 2003, and 2008, respectively. He also attained the status of Professional Engineer (P.E.Jp) in electrical and electronic engineering in 2009.

In 2003, he joined NTT Access Network Service Systems Laboratories, Ibaraki, Japan. He has been engaged in the research on optical fiber design and measurement. He is a member of the Institute of Electronics, Information and Communication Engineers (IEICE) of Japan. He received the Young Researcher's Award from the IEICE in 2008 and Japanese Ministry of Economy, Trade and Industry (METI) international standardization encourage award in 2014.

**Yuto Sagae** received the B.E. and M.E. degrees from Tohoku University, Miyagi, Japan, in 2013 and 2015, respectively. In 2015, he joined NTT Access Network Service Systems Laboratories, NTT, Ibaraki, Japan, where he has been researching optical fiber designs. He is a member of the Institute of Electronics, Information and Communication Engineers. He received the Best Paper Award in OECC/PS 2019.

**Taiji Sakamoto** received the B.E., M.E., and Ph.D. degrees in electrical engineering from Osaka Prefecture University, Osaka, Japan, in 2004, 2006, and 2012, respectively. In 2006, he joined NTT Access Network Service Systems Laboratories, NTT, Ibaraki, Japan, where he has been engaged in researching optical fiber nonlinear effects, low nonlinear optical fiber, few-mode fiber, and multi-core fiber for optical MIMO transmission systems. He is a member of the Institute of Electronics, Information and Communication Engineers.

**Kazuhide Nakajima** (Member, IEEE) received the M.S. and Ph.D. degrees in electrical engineering from Nihon University, Chiba, Japan, in 1994 and 2005, respectively. In 1994, he joined NTT Access Network Systems Laboratories, Tokai, Ibaraki, Japan, where he was engaged in the research on optical fiber design and related measurement techniques.

He is currently a Group Leader (Senior Distinguished Researcher) with NTT Access Network Service Systems Laboratories, Tsukuba, Ibaraki, Japan. He is acting as a Rapporteur of Q5/SG15 of ITU-T since 2009. He is a member of the the Optical Society (OSA), the Institute of Electronics, Information and Communication Engineers (IEICE) of Japan, and the Japan society of applied physics (JSAP). He received the Best Paper Award in OECC'96, the Best Paper Award in IEICE'11, the Achievement Award in IEICE'12, and the Maejima Hisoka Award in 2016.